

# In Vivo Imaging of Secondary Neurodegeneration Associated With Phosphatidylserine Externalization Along Axotomized Axons

Fan Yang,<sup>1</sup> Mohammadali Almasieh,<sup>1</sup> and Leonard A. Levin<sup>1,2</sup>

<sup>1</sup>Department of Ophthalmology and Visual Sciences, McGill University, Montreal, Canada

<sup>2</sup>Department of Neurology and Neurosurgery, McGill University, Montreal, Canada

Correspondence: Leonard A. Levin, Montreal Neurological Institute, 3801 University St., Room MP116, Montreal QC H3A 2B4, Canada; [leonard.levin@mcgill.ca](mailto:leonard.levin@mcgill.ca).

Received: July 21, 2023

Accepted: December 11, 2023

Published: February 12, 2024

Citation: Yang F, Almasieh M, Levin LA. In vivo imaging of secondary neurodegeneration associated with phosphatidylserine externalization along axotomized axons. *Invest Ophthalmol Vis Sci.* 2024;65(2):24. <https://doi.org/10.1167/iovs.65.2.24>

**PURPOSE.** Axonal degeneration in acute and chronic disorders is well-characterized, comprising retrograde (proximal) and Wallerian (distal) degeneration, but the mechanism of propagation remains less understood.

**METHODS.** Laser injury with a diode-pumped solid-state 532 nm laser was used to axotomize retinal ganglion cell axons. We used confocal in vivo imaging to demonstrate that phosphatidylserine externalization is a biomarker of early axonal degeneration after selective intraretinal axotomy.

**RESULTS.** Quantitative dynamic analysis revealed that the rate of axonal degeneration was fastest within 40 minutes, then decreased exponentially afterwards. Axonal degeneration was constrained within the same axotomized axonal bundles. Remarkably, axon degeneration arising from the site of injury induced a secondary degeneration of distal normal axons.

**CONCLUSIONS.** Axonal degeneration in vivo is a progressive process associated with phosphatidylserine externalization, which can propagate not only along the axon but to adjacent uninjured axons. This finding has implications for acute and chronic neurodegenerative disorders associated with axonal injury.

Keywords: axonal degeneration, confocal scanning laser ophthalmoscopy, phosphatidylserine

Axonal degeneration is an extensively and well-characterized event in many neurodegenerative disorders, including glaucoma, optic neuropathies, stroke, and multiple sclerosis.<sup>1</sup> Axonal degeneration typically progresses from the primary injury site along the axons in two directions, one toward the soma (retrograde degeneration) and the other toward the distal axonal synaptic terminals (Wallerian degeneration). Axonal degeneration in both acute injuries and chronic neurodegenerative disorders share similar morphological structural alterations, namely, retrograde degeneration and Wallerian degeneration, indicating a shared mechanism for neuronal and axonal self-destruction in acute traumatic injuries and chronic degenerative disorders.<sup>2,3</sup>

Phosphatidylserine (PS) is an essential component of cell membranes in prokaryotic and eukaryotic cells. Dynamic translocation of PS from the inner to the outer membrane leaflet (i.e., externalization) is a vital process in development, oncogenesis, neurodegeneration, and regeneration.<sup>4,5</sup> We previously demonstrated that PS externalization is an early stage of axonal degeneration after axonal injury, based on in vitro studies using single-axon ultrafast laser axotomy of purified rat retinal ganglion cells (RGCs).<sup>6</sup> PS externalization starts within minutes after axonal injury, and is followed 30 minutes later by morphological evidence (e.g., beading) of axonal degeneration. The mechanism of PS externaliza-

tion is redox-sensitive and is slowed in the Wallerian degeneration slow rat or by intracellular delivery of a disulfide reducing agent.

The above studies of PS externalization in axons were performed in vitro.<sup>6</sup> However, the spatial and temporal nature of PS externalization along injured RGC axons has not been studied to the same extent in vivo because its quantification is challenging. To carry out in vivo studies, we took advantage of the ability to directly visualize RGC axons in the retinal nerve fiber layer of the living eye using confocal scanning laser ophthalmoscopy (CSLO) and optical coherence tomography (OCT).<sup>7</sup> This imaging was coupled with tools to focally injure RGC axons using a continuous-wave laser and subsequently monitoring the labeled axonal membrane PS with a polarity-sensitive annexin-based biosensor with switchable fluorescence states.<sup>8,9</sup>

## METHODS

### Experimental Animals

Animals (n = 116) used in this study were treated in accordance with the guidelines of the Canadian Council on Animal Care, the Association for Research in Vision and Ophthalmology, and approved institutional protocols. Female 10- to 12-week-old Long-Evans rats weighing 180



to 200 g (Charles River Laboratories, Wilmington, MA, USA) were maintained in standard housing with white paper bedding. The environment was kept at 21°C with a 12-hour light and 12-hour dark cycle. All animals were fed as desired.

All procedures (injection, surgery, and imaging) were performed under anesthesia and in aseptic conditions. Rodent cocktail solution containing ketamine (50 mg/mL), xylazine (5 mg/mL), and acepromazine (1 mg/mL) was injected intraperitoneally at 0.1 mL per 100 g body weight for anesthesia. A supplementary dose was applied when necessary for longer durations of imaging. Erythromycin ophthalmic ointment was applied to both eyes after all procedures to prevent damage to the cornea, and sterile saline solution at 5.0 mL per 100 g body weight was injected subcutaneously to prevent dehydration. After procedures animals were placed in warmed recovery cages and closely monitored until the return of normal behavior, at which point they were transferred to their home cages.

### CSLO and OCT

CSLO and OCT were performed with a Spectralis HRA+OCT (Heidelberg Engineering GmbH, Heidelberg, Germany). CSLO and OCT are noninvasive and noncontact methods for imaging axons and retinal layer morphology within the retina, either en face or in cross-section. Under anesthesia, animal pupils were dilated with topical tropicamide 2.5% and phenylephrine 0.5%. A rat contact lens (no. 553632; Cantor & Nissel, Brackley, UK) was placed on the eye. The animal was then positioned in front of the CSLO using an animal imaging platform based on an optic bench (Thorlabs, Newton, NJ, USA). A series of normal baseline fundus images were acquired with blue reflectance imaging (BR), infrared reflectance imaging (IR), blue laser autofluorescence imaging (BAF), and OCT. Line scan images were acquired in high resolution mode, 30° field of view, 1536 × 1536 pixels, and with automatic real time-function averaging at 100 samples, less if there was breathing or other movement artifact that necessitated faster acquisition.

### Intravitreal Injection of Phosphatidylserine-Specific Fluorescent Probe

The fluorescent probe pSIVA linked to *N,N*-di-methyl-*N*-(iodoacetyl)-*N*-(7-nitrobenz-2-oxa-1,3-diazol-4-yl)ethylene amine (pSIVA-IANBD; NBP2-29382; Novus Biologicals, Centennial, CO, USA) was used to detect phosphatidylserine (PS) externalization along the RGC axonal membrane.<sup>8</sup> Intravitreal injections of the probe were performed under the surgical microscope immediately posterior to the superotemporal limbus. After the sclera was penetrated with a 30-gauge needle at a 45° angle, a 32-gauge needle was attached to a 5 µL Hamilton syringe (Hamilton, Reno, NV, USA) for injection. This location of puncture and entry route of administration helps avoiding both retinal detachment and injury to the lens. A 4 µL volume was slowly injected over a 60-second period. The needle was held in place for another 60 seconds, then slowly withdrawn. The injection perforation was sealed by application of small amount of surgical tissue adhesive glue (3M Vetbond, St. Paul, MN, USA). Dextran-fluorescein of 40,000 MW (catalog D1844; ThermoFisher, Hillsboro, OR, USA) was used as a non-PS binding control for injections.

## Laser Intraretinal Axotomy

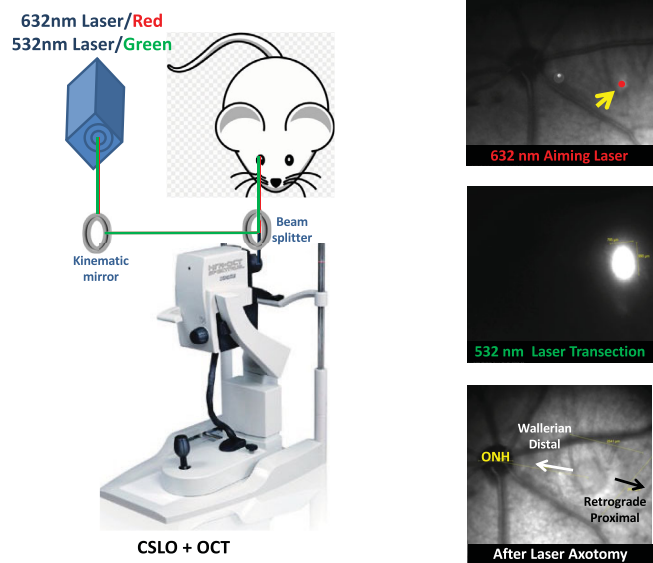


**FIGURE 1.** Intraretinal laser transection of retinal ganglion cell axons. A low-power 632 nm laser is used to focus on an area of retina away from large retinal vessels. A 100 mW 532 nm laser beam is then used to achieve axonal transection. ONH, optic nerve head.

### Intraretinal Axotomy

After intravitreal injection of the PS-specific probe, the animal was positioned on a platform in front of the CSLO, and the fundus of the eye was examined for any procedure-related complications. Then, while monitored in real-time by CSLO, a targeting red laser (632 nm at 5 mW) was projected through a 50% transmission split filter to assist in aiming at the selected axon bundles of retina to be transected (Fig. 1). A diode-pumped solid-state 532 nm 200 mW laser (Laserglow Technologies, Toronto, ON, Canada) green laser was then projected through 1% transmission filters to fine-tune the aiming. Finally, intraretinal axotomy of selected RGC axon bundles was induced with computer-control (LabVIEW, National Instruments, TX, USA) of the green laser at 100 mW for 15 seconds. Beginning immediately after axotomy and for the next 300 minutes, the progression of PS externalization along the injured axons was monitored and images acquired by CSLO.

In some animals, two additional lower-power laser injuries of 50 mW for 15 seconds were aimed adjacent but not contiguous to the 100 mW site, either in the same direction of the nerve fiber layer under the 100 mW site or separate from it. The 50 mW power was chosen because preliminary experiments demonstrated that it did not result in axotomy-induced PS externalization.

### CSLO Imaging Analysis

Images were analyzed and quantified manually using Heidelberg Eye Explorer (HEYEX) software (Spectralis HRA+OCT v5.8; Heidelberg Engineering GmbH). The progression in the length of the fluorescent probe-labelled PS signal in acquired images was measured from the center of the laser axotomy site to the maximal extent in the proximal and distal axon bundles (Supplemen-

tary Fig. S1). This allowed determination of any differential effects of laser axotomy on retrograde degeneration (toward the retinal ganglion cell bodies along the proximal axon) and Wallerian degeneration (away from the cell body along the distal axon). This measurement of the length of the PS signal was performed in a masked fashion by a single investigator (F.Y.) to reduce variability, followed by confirmation of measurements by all investigators (F.Y., M.A., L.A.L.) via a Zoom review of the images to ensure that the longest axon bundle was measured in each direction. The entire length of the proximal and distal fluorescent probe-labeled PS signal at every time point was summed. The measured values of maximal length and the time needed for the half-maximal length were then calculated, derived, and graphed using Microsoft Excel.

### Retinal Wholemounts

To verify the accuracy of the observed PS labeling in vivo by CSLO, retinal wholemounts were studied at the end of the experiment for each animal. Briefly, animals were euthanized, the eyes were enucleated and fixed overnight in 4% paraformaldehyde at room temperature, and the retinas were dissected under a surgical microscope and thoroughly rinsed with phosphate-buffered saline solution. Each retina was mounted vitreous side up on a glass slide, and

antifade mounting medium was applied and then covered and sealed with a glass coverslip. Images were acquired by fluorescence microscopy with an Olympus IX83 inverted microscope.

### Statistical Analysis

Values were reported as mean  $\pm$  standard deviation (SD). Repeated-measures analysis of variance or paired Student *t*-testing was used for statistical analysis using JMP statistics software (SAS, Cary, NC, USA). *P* value < 0.05 was considered statistically significant.

## RESULTS

### Phosphatidylserine Externalization In Vivo After Acute Axonal Injury

Fluorescence-based in vivo confocal imaging identified axonal PS externalization measured with IANBD-annexin B12 along the injured axonal membrane within a few minutes after intraretinal laser injury to retinal nerve fiber bundles (Fig. 2). PS externalization was detected both distal and proximal to the site of injury, and progressed over time along a longitudinal orientation of the axon bundles. In contrast, no detectable PS externalization was identified in somas or dendrites of RGCs at any imaging session,

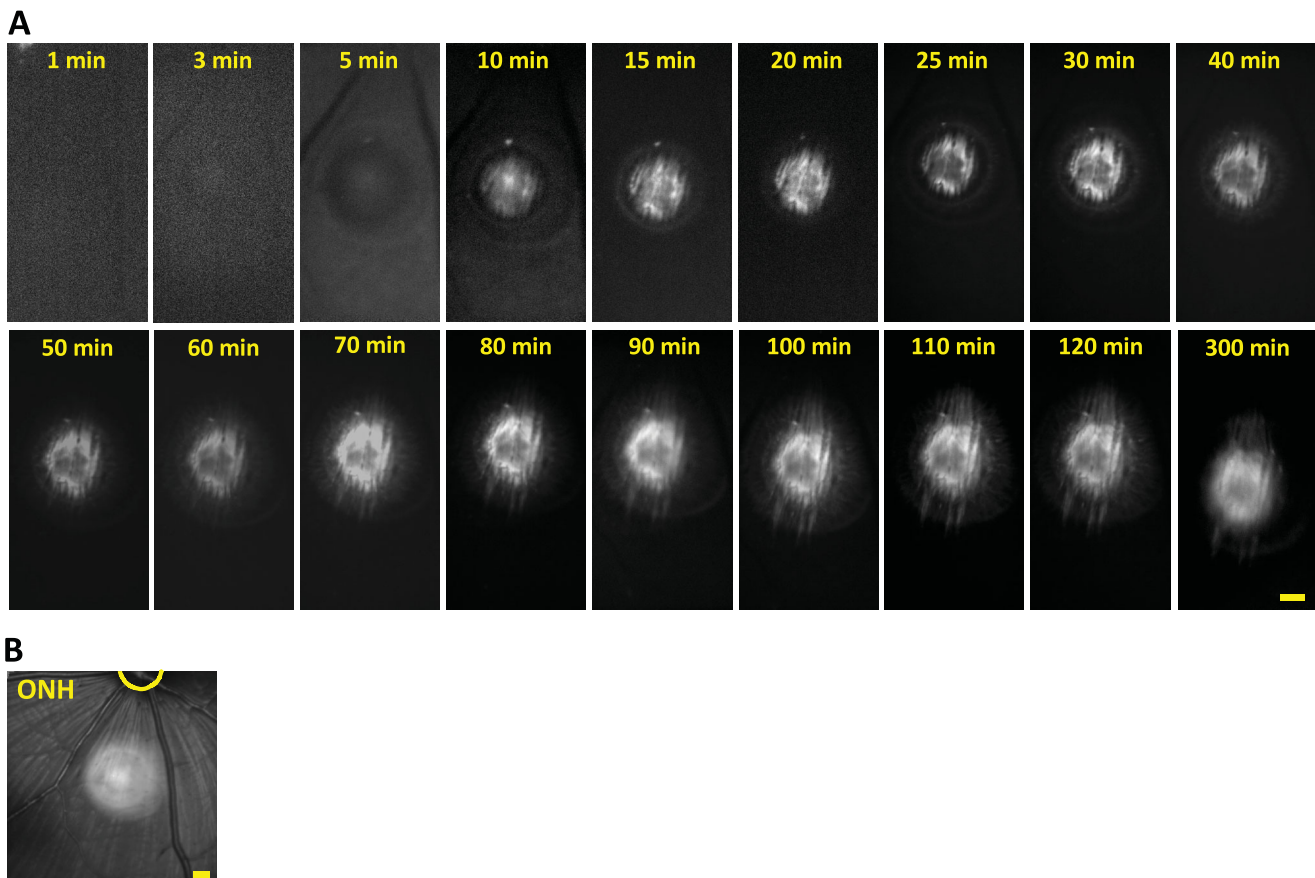


**FIGURE 2.** Spatial and temporal externalization of axonal PS after intraretinal laser axotomy. **(A)** The expansion of PS externalization along the injured retinal axons was continually monitored for 300 minutes after intraretinal laser axotomy. Images are IANBD fluorescence elicited by 488 nm laser excitation. **(B)** A representative polarization-sensitive reflectance image displays the location of intraretinal laser axotomy, acquired nine minutes after injury. Scale bar: 500  $\mu$ m.



including after a second intravitreal injection of the fluorescent probe at 24 hours. These results suggest that somas and dendrites do not display apoptotic-type degeneration or fragmentation during the early phase after axonal injury, consistent with previous reports demonstrating dendritic or somal degeneration only days to weeks after injury or later.<sup>10</sup> No axonal fluorescence was seen in animals that either did not receive injections or in animals injected with a control fluorophore, dextran-fluorescein of similar molecular weight to IANBD-annexin B12 (Supplementary Figs. S2 and S3).

OCT imaging of the site of laser injury demonstrated retinal edema with thickening of all retinal layers (Fig. 3). The normal thickness of the rat retina before laser injury is  $201 \pm 9 \mu\text{m}$  ( $N = 11$ , mean  $\pm$  SD), and significantly increased to  $233 \pm 13 \mu\text{m}$  ( $P < 0.004$ ) by five minutes after laser axotomy, and to  $335 \pm 39 \mu\text{m}$  ( $P < 0.0001$ ) by 300 minutes. The edema was round and radially symmetric, consistent with the shape of the laser spot. The diameter of the edema was  $\sim 1137 \mu\text{m}$  by five minutes after laser axotomy, and it expanded gradually to  $1655 \mu\text{m}$  by 300 minutes. PS externalization only propagated along the course of the injured axons and not transversely.

### Dynamic Profile of Phosphatidylserine Externalization In Vivo After Acute Axonal Injury

The spatial and temporal characteristics of PS externalization in vivo after acute axonal injury were quantified by measuring the length of axonal fluorescence along the nerve fiber bundle over time (Fig. 4A). PS externalization along lesioned axons reached a plateau 300 minutes after axonal injury. The half maximum point was reached 40 minutes after axonal injury. The initial rate of axonal degeneration in vivo for the first 40 minutes was  $18 \mu\text{m}/\text{min}$ , then the rate decreased significantly to  $6 \mu\text{m}/\text{min}$  between 40 to 80 min, and then to  $1.6 \mu\text{m}/\text{min}$  between 80 to 300 min (Fig. 4B). There was no increase in the amount of PS externalization when retinas were reimaged after 24 hours, even when a second intravitreal injection of pSIVA probe was applied to ensure sufficient ligand for labeling the externalized phosphatidylserine.

To confirm that the in vivo CSLO imaging fairly represented what was occurring in RGC axons, the length of

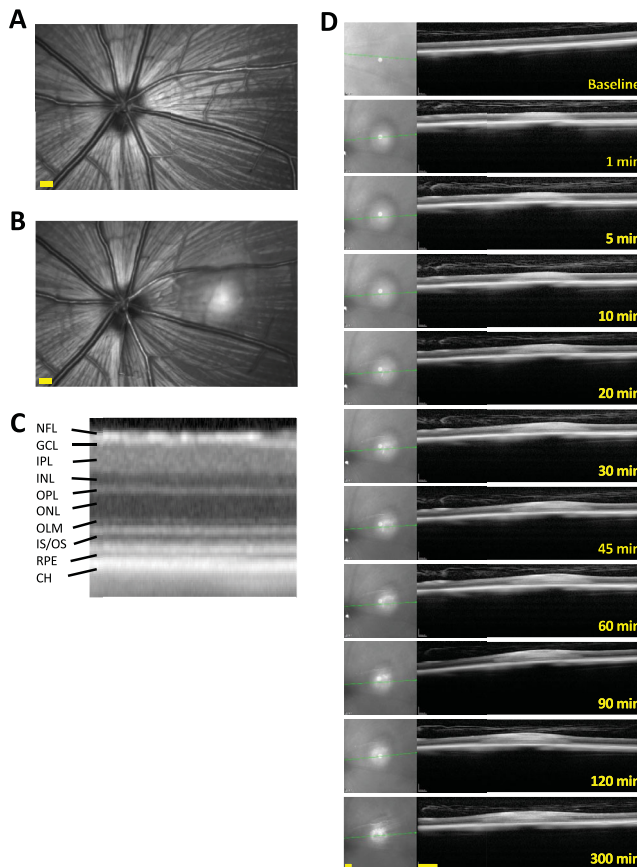


FIGURE 3. The spatial and temporal alteration of gross retinal morphology detected by OCT after intraretinal laser axotomy. (A) A representative polarization-sensitive image demonstrates normal baseline retinal axons before intraretinal axotomy. (B) A representative polarization-sensitive image of the same rat immediately after intraretinal laser axotomy. (C) A representative OCT image demonstrates normal retinal layers. (D) Serial CSLO and OCT imaging of retinal morphology from before axotomy to 300 minutes after intraretinal laser axotomy. Scale bar:  $500 \mu\text{m}$ . NFL, nerve fiber layer; GCL, ganglion cell layer; IPL, inner plexiform layer; INL, inner nuclear layer; OPL, outer plexiform layer; ONL, outer nuclear layer; OLM, outer limiting membrane; IS/OS, inner/outer segment junctions; RPE, retinal pigment epithelium; CH, choroid.

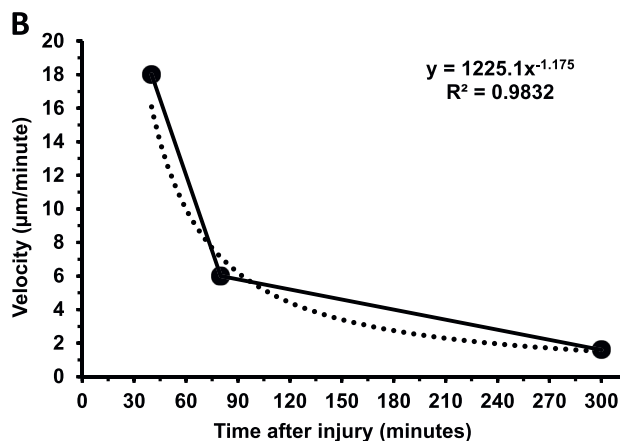
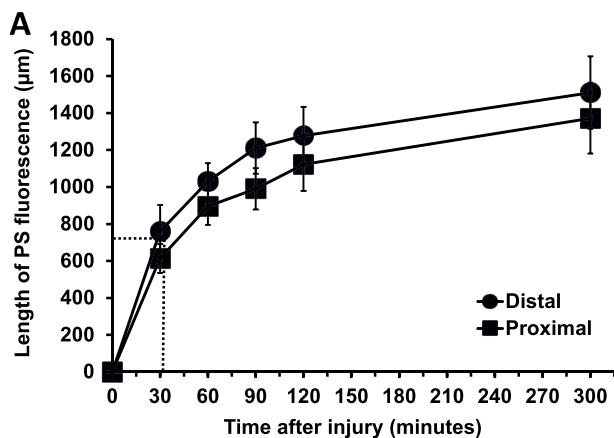
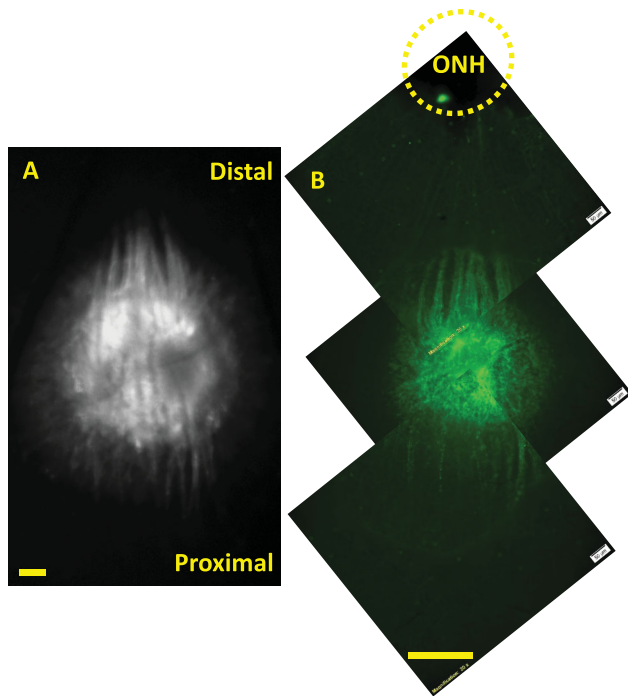
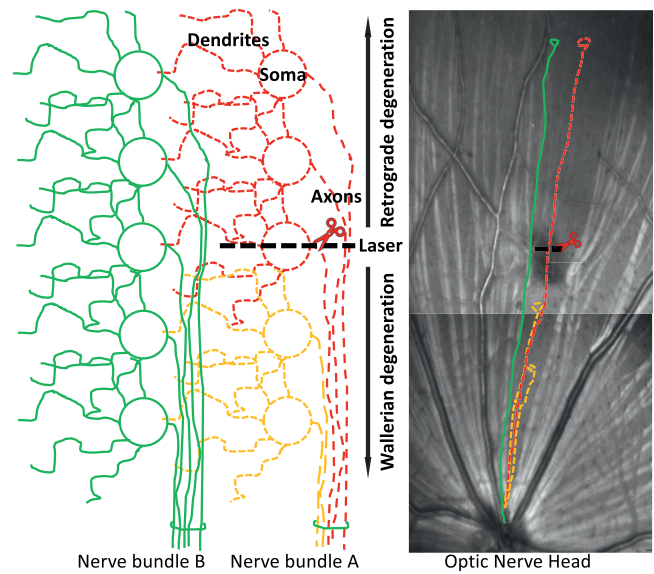


FIGURE 4. The dynamic externalization of PS along the retinal axons after retinal laser axotomy. (A) Acute progressive externalization of PS along injured retinal axons after retinal axotomy ( $n = 7$ , mean  $\pm$  SEM, error bars indicate the SEM). The externalization of PS along the injured axons plateaued after axotomy, and the time reaching the half maximum velocity was at approximately 40 minutes. (B) The velocity PS externalization along injured axons decreased exponentially from  $18 \mu\text{m}$  to  $6 \mu\text{m}$  from 40 to 80 minutes, and from  $6 \mu\text{m}$  to less than  $1.3 \mu\text{m}$  from 80 to 300 minutes.  $*P < 0.05$ ,  $**P < 0.01$  ( $n = 14$ , pooled 7 distal and 7 proximal).



**FIGURE 5.** Pattern of PS externalization observed in vivo using confocal scanning laser ophthalmoscopic fluorescence imaging is identical to that seen ex vivo in retinal whole mounts. (A) Representative pattern of PS externalization along injured retinal axons observed in vivo with fluorescence imaging by CSLO. (B) Representative pattern of PS externalization along injured retinal axons observed ex vivo in a retinal wholemount of the same retina as in A, using the same IANBD-pSIVA PS probe. ONH, optic nerve head. Scale bar: 500  $\mu$ m.

labeled PS externalization was verified 300 minutes after injury by ex vivo examination of retinal wholemounts using fluorescent microscopy. The results of the imaging acquired by in vivo (Fig. 5A) and by fluorescent microscopy ex vivo (Fig. 5B) were nearly identical, both in terms of the area of laser-induced morphological changes and the length of the PS externalization-labeled nerve bundles using the pSIVA probe.



**FIGURE 7.** Schematic of primary and secondary retinal axonal degeneration after intraretinal laser axotomy. Intraretinal laser axotomy induced primary axonal degeneration (red somas and axons), which progressively induced secondary axonal degeneration in axons of uninjured RGC axons within the same axonal bundle (yellow). In contrast, primary and secondary axonal degeneration did not affect axons within adjacent bundles (green). The depicted polarization-sensitive imaging of axonal bundles was acquired 105 days after laser axotomy.

### Laser-Induced Axotomy Causes Secondary Axonal Degeneration in Adjacent Uninjured Axons

Acute axonal injury induced with laser axotomy result in the degeneration of lesioned axons over time, as by the gradual disappearance from day 7 to day 10 of retinal axonal nerve bundles proximal to the laser lesion (Fig. 6). Surprisingly, the axonal nerve bundles on the distal side of the lesion also degenerated, even though they contain a mix of axons, some axotomized but other not directly injured by the laser axotomy because their RGC somas were distal to the laser injury. A schematic drawing (Fig. 7) depicts how the primary axotomy (to red axons) induces axonal degeneration.

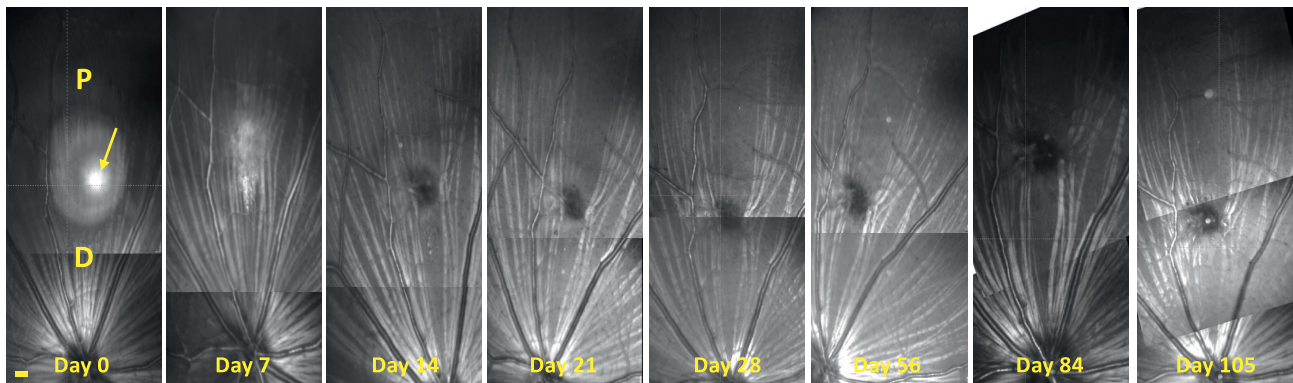


**FIGURE 6.** Intraretinal laser axotomy induces progressive axonal degeneration in uninjured axons. Monitoring the injured bundles over time by in vivo imaging of retinal axons proximal (P) and distal (D) to the laser axotomy site (arrow) demonstrates progressive axonal degeneration in both directions. The axons proximal to the injury project from proximal RGC somas, and therefore all are axotomized. The axons distal to the injury site include axons from both proximal and distal RGC somas, and therefore a mixture of axotomized and non-axotomized axons. Scale bar: 500  $\mu$ m.



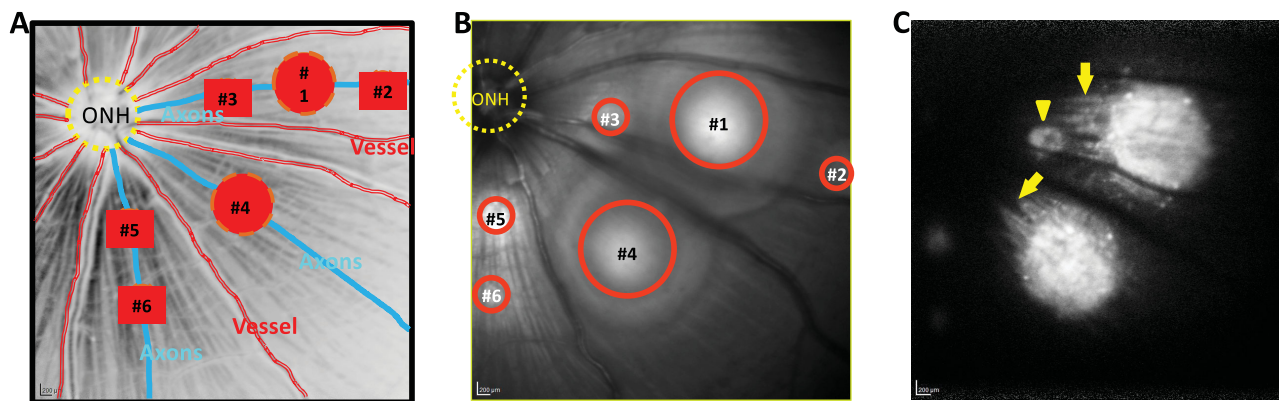


**FIGURE 8.** Effect of adjacent low-intensity laser injury on PS externalization after a high-intensity injury. (A) The retina is overlaid with the locations of six retinal laser injuries (red discs) to three retinal axonal bundles (blue lines). The number on the disc represents the sequence of laser delivery, with the larger red discs representing higher laser power and the smaller red discs representing lower laser power. (B) The result of retinal injury after laser, based on polarization-sensitive imaging, and indicated by six red circles. (C) The expansion and interactions of PS externalization between the larger and the smaller laser injuries were simultaneously identified by fluorescence imaging 300 minutes after intraretinal laser axotomy. Yellow arrows depict labeling of externalized PS towards the ONH. The yellow triangle depicts a second low-energy laser injury (#3) along the course of the damaged axons of #1. #5 and #6 are control burns to axon bundles separate from the other primary burn (#4). ONH, optic nerve head.

eration in both injured (red axons) and uninjured retinal axons (yellow axons). The spread of injury from the primarily injured axons did not involve adjacent bundles (green axons), indicating that the factor(s) responsible was did not diffuse far from the axotomy site.

### Plateau of Phosphatidylserine Externalization Along Injured Axons Is Likely Due to Decreased Access of IANBD-Annexin B12 to Axons

There was a substantial decrease in the velocity of PS externalization propagation along the axon in vivo (Fig. 4). This was different from what we previously observed when isolated RGC axons were axotomized in vitro.<sup>6</sup> We hypothesized that the decrease in propagation in vivo was related to access of the fluorescent pSIVA-IANBD annexin probe to the axon and not to an actual decrease in velocity of PS externalization. To test this hypothesis, we performed low-power laser injuries adjacent to laser injuries that were of sufficient power to cause axotomy. We compared the effect on PS propagation when the low-power injuries were *along* the course of the axotomized axons to those that were *separate from* the axotomized axons (Figs. 8A, 8B). We found that the propagation of axonal PS externalization continued along the axonal bundles from the axotomy injury when a low-power burn (insufficient to cut axons) was in the same trajectory (along the same bundles), but not when it was separate (Fig. 8C). This result is consistent with the low-power laser injury increasing access of the pSIVA-IANBD PS probe to the axons that were axotomized, and not to an actual inhibition of propagation over time.

## DISCUSSION

This study took advantage of the ability to noninvasively image CNS axons via the clear optical path through the eye to the retina, demonstrating progressive externalization of PS along bundles of RGC axons after focal injury. These in vivo findings extend our previous in vitro demonstration

of PS externalization after ultrashort laser injury to axons in purified RGC cultures.<sup>6</sup> In that study we showed propagation of the externalization at a velocity of approximately 10  $\mu\text{m}/\text{min}$  proximal and distal to the injury site, and that the propagation is redox-sensitive. In the present study, we demonstrate that PS externalization occurs along RGC axons in vivo at approximately the same rate as found in our in vitro study. We also found evidence for a plateau in the velocity of PS externalization in vivo, going from 18  $\mu\text{m}/\text{min}$  to 1.6  $\mu\text{m}/\text{min}$  over the course of the 300-minute observation time. In addition, the propagation of PS externalization eventually halted.

There are two possibilities which could explain the apparent slowing of propagation of PS externalization over time in vivo. First, the in vivo situation fundamentally differs from in vitro, and PS externalization does not occur. If this is the case, then perhaps the in vitro observations could be related to the specific nature of how the experiments were performed. For example, immunopurified RGCs were studied in a chemically defined medium containing multiple neurotrophins and other growth factors. There were no amacrine, bipolar, and glial cells in the cultures, different from the normal milieu of an RGC. A second possibility is that the externalization continues at the same velocity but that it becomes difficult to detect because of the use of the IANBD-annexin B12 probe. This probe is designed to become fluorescent when it intercalates into axonal membranes, but such intercalation would become more difficult if the probe does not penetrate the retinal internal limiting membrane, a basement membrane containing several extracellular matrix proteins. The laser injury itself is of sufficient power to cause thermal injury to all layers of the retina, based on OCT (Fig. 3), and thus only the area of the laser and the immediately adjacent retina would disrupt the inner limiting membrane (ILM).

To differentiate these two reasons for limited progression of PS externalization in vivo, after 300 minutes, we injured areas of the retina adjacent to the primary injury with secondary laser of insufficient power to cause detectable axonal injury. This lower power was chosen to allow increased access of the PS-detecting fluorophore by

disrupting the ILM, but without cutting the axons immediately below. The results (Fig. 8) demonstrated that when a subthreshold laser injury was adjacent to a suprathreshold laser injury, the amount of propagation of the detected PS externalization along axons was greatest when the subthreshold injury was along the course of the same axons as those traversing the suprathreshold injury. In contrast, when the axons traversing the subthreshold injury were separate from those traversing the suprathreshold injury, there was less propagation of PS externalization. This result is consistent with the mechanism explaining the plateau in propagation of PS externalization in vivo being a limited availability of the probe at the axons, and not a failure of propagation. However, the results do not prove that the increased extension of PS propagation with low-power laser energy is the result of disruption of the ILM. The issue of limited access of PS probe to axons is moot for in vitro studies because there is no ILM in cultures and the axons are bare.

Given those findings, we considered using various enzymes to disrupt the internal limiting membrane. We focused on attempting the use of low-dose pronase E, given published research that papain and collagenase were associated with retinal morphological changes and effects on reactive gliosis.<sup>11</sup> However, even with pronase E we were unsuccessful in being able to image PS propagation far beyond the area of laser injury, and given that the ILM was not directly imaged, this does not bear light on the role of the ILM in preventing access of the probe to the axon. Future studies, perhaps using transgenic-based detection methods, may better demonstrate the degree of PS propagation in axons away from the injury site.

The other main outcome of this study was the surprising finding that in the involved bundles, *all* axons between the axotomy site and the optic nerve head underwent degeneration, including those whose somas were distal to the axotomy and thus not injured by the laser (Figs. 6 and 7). This complete loss of axons indicates that there was axon-to-axon secondary degeneration, from, primarily injured axons to adjacent uninjured axons. Secondary degeneration is a well-studied phenomenon, including axon-to-axon secondary degeneration.<sup>12–19</sup> We have modeled the effects of secondary degeneration in understanding the spread of injury in Leber hereditary optic neuropathy.<sup>20,21</sup> However, the mechanisms for axonal secondary degeneration in this model is unclear and could be due to reactive oxygen species or other diffusible mediators.<sup>20,21</sup> It is also possible that the spread of axonal injury is related to PS externalization, which is an “eat-me” signal for macrophages or other phagocytic cells.<sup>22,23</sup> An activation of phagocytosis of primarily injured axons could result in a bystander effect for adjacent axons within the same axonal bundle.

### Phosphatidylserine Externalization Is a Biomarker of Early Axonal Degeneration In Vivo After Acute Axonal Injury

Detection of early axonal degeneration in vivo is challenging, and few studies have specifically explored RGC degeneration. Most degeneration is detected after days to weeks, when it would be too late to initiate treatment because RGCs and their axons are already in the irreversible stage of degeneration (e.g., axonal beading and fragmentation). Detecting early neurodegeneration could provide critical information for a better understanding the molecular and cellular mecha-

nisms underlying the pathogenesis, progression, and regeneration of axonal degeneration. Detection methods might also have clinical application for early diagnosis, and consequently early treatment, of axonal diseases such as glaucoma.

In summary, we demonstrated PS externalization along axon bundles in the retinal nerve fiber layer within minutes of acute intraretinal laser axotomy, using noninvasive fluorescence-based in vivo confocal imaging. The fluorescent-labeled PS externalization progressed bidirectionally towards proximal and distal segments of the axon at the same rate. Loss of uninjured axons distal to the axotomy site indicates the presence of focal secondary axonal degeneration. Detection of externalized PS in vivo is therefore a biomarker of ongoing axonal *damage*, separate from axonal *loss* measured by techniques such as OCT. If high-sensitivity PS-binding molecules could be adapted for use in the clinical arena, then potentially this method could be used to monitor disease activity, gauge the effectiveness of ongoing treatments, and potentially predict disease prognosis.

### Acknowledgments

Supported by the Canadian Institutes for Health Research, Canadian Foundation for Innovation, Canada Research Chairs, National Institutes of Health.

Disclosure: **F. Yang**, None; **M. Almasieh**, None; **L.A. Levin**, Annexon (C), Eyevegensys (C), Genentech (C), Janssen (C), Perfuse (C), Prilena (C), Roche (C), Santen (C), UNITY (C), Wisconsin Alumni Research Foundation (P)

### References

- Hughes RO, Bosanac T, Mao X, et al. Small molecule SARM1 inhibitors recapitulate the SARM1(–/–) phenotype and allow recovery of a metastable pool of axons fated to degenerate. *Cell Rep.* 2021;34:108588.
- Waller AV. Experiments on the section of glossopharyngeal and hypoglossal nerves of the frog, and observations on the alterations produced thereby in the structure of their primitive fibers. *Philos Trans R Soc London B Biol Sci.* 1850;140:423–429.
- Schwartz M, Yoles E, Levin LA. ‘Axogenic’ and ‘soma-genic’ neurodegenerative diseases: definitions and therapeutic implications. *Mol Med Today.* 1999;5:470–473.
- van den Eijnde SM, van den Hoff MJ, Reutelingsperger CP, et al. Transient expression of phosphatidylserine at cell-cell contact areas is required for myotube formation. *J Cell Sci.* 2001;114:3631–3642.
- Martin SJ, Reutelingsperger CP, McGahon AJ, et al. Early redistribution of plasma membrane phosphatidylserine is a general feature of apoptosis regardless of the initiating stimulus: inhibition by overexpression of Bcl-2 and Abl. *J Exp Med.* 1995;182:1545–1556.
- Almasieh M, Catrinescu MM, Binan L, Costantino S, Levin LA. Axonal degeneration in retinal ganglion cells is associated with a membrane polarity-sensitive redox process. *J Neurosci.* 2017;37:3824–3839.
- Kanamori A, Catrinescu MM, Traistaru M, Beaubien R, Levin LA. In vivo imaging of retinal ganglion cell axons within the nerve fiber layer. *Invest Ophthalmol Vis Sci.* 2010;51:2011–2018.
- Kim YE, Chen J, Chan JR, Langen R. Engineering a polarity-sensitive biosensor for time-lapse imaging of apoptotic processes and degeneration. *Nat Methods.* 2010;7:67–73.

9. Kim YE, Chen J, Langen R, Chan JR. Monitoring apoptosis and neuronal degeneration by real-time detection of phosphatidylserine externalization using a polarity-sensitive indicator of viability and apoptosis. *Nat Protoc*. 2010;5:1396–1405.
10. Leung CK-s, Weinreb RN, Li ZW, et al. Long-term in vivo imaging and measurement of dendritic shrinkage of retinal ganglion cells. *Invest Ophthalmol Vis Sci*. 2011;52:1539–1547.
11. Zhang KY, Tuffy C, Mertz JL, et al. Role of the internal limiting membrane in structural engraftment and topographic spacing of transplanted human stem cell-derived retinal ganglion cells. *Stem Cell Reports*. 2021;16:149–167.
12. Yoles E, Muller S, Schwartz M. NMDA-receptor antagonist protects neurons from secondary degeneration after partial optic nerve crush. *J Neurotrauma*. 1997;14:665–675.
13. Moalem G, Leibowitz-Amit R, Yoles E, Mor F, Cohen IR, Schwartz M. Autoimmune T cells protect neurons from secondary degeneration after central nervous system axotomy. *Nat Med*. 1999;5:49–55.
14. Levkovitch-Verbin H, Quigley HA, Kerrigan-Baumrind LA, D'Anna SA, Kerrigan D, Pease ME. Optic nerve transection in monkeys may result in secondary degeneration of retinal ganglion cells. *Invest Ophthalmol Vis Sci*. 2001;42:975–982.
15. Levkovitch-Verbin H, Quigley HA, Martin KR, Zack DJ, Pease ME, Valenta DF. A model to study differences between primary and secondary degeneration of retinal ganglion cells in rats by partial optic nerve transection. *Invest Ophthalmol Vis Sci*. 2003;44:3388–3393.
16. Blair M, Pease ME, Hammond J, et al. Effect of glatiramer acetate on primary and secondary degeneration of retinal ganglion cells in the rat. *Invest Ophthalmol Vis Sci*. 2005;46:884–890.
17. Fitzgerald M, Bartlett CA, Harvey AR, Dunlop SA. Early events of secondary degeneration after partial optic nerve transection: an immunohistochemical study. *J Neurotrauma*. 2010;27:439–452.
18. Li HY, Ruan YW, Ren CR, Cui Q, So KF. Mechanisms of secondary degeneration after partial optic nerve transection. *Neural Regen Res*. 2014;9:565–574.
19. Stirling DP, Cummins K, Wayne Chen SR, Stys P. Axoplasmic reticulum Ca(2+) release causes secondary degeneration of spinal axons. *Ann Neurol*. 2014;75:220–229.
20. Coussa RG, Merat P, Levin LA. Propagation and selectivity of axonal loss in Leber hereditary optic neuropathy. *Sci Rep*. 2019;9:6720.
21. Lambiri DW, Levin LA. Modeling reactive oxygen species-induced axonal loss in Leber hereditary optic neuropathy. *Biomolecules*. 2022;12:1411.
22. Faris H, Almasieh M, Levin LA. Axonal degeneration induces distinct patterns of phosphatidylserine and phosphatidylethanolamine externalization. *Cell Death Discov*. 2021;7:247.
23. Almasieh M, Faris H, Levin LA. Pivotal roles for membrane phospholipids in axonal degeneration. *Int J Biochem Cell Biol*. 2022;150:106264.